PHYSICAL REVIEW B VOLUME 26, NUMBER 12 15 DECEMBER 1982

Electrodynamic response of a bounded electron gas in hydrodynamic formalism: Theory and applications

S. Das Sarma
Center for Theoretical Physics, Department of Physics and Astronomy, University of Maryland, College Park, Maryland 20742
(Received 2 February 1982)

Coupled integral equations for the electrodynamic response of a bounded electron gas are written down within a unified hydrodynamical model. The nonretarded limit of the formalism is considered in detail and the induced density fluctuation is expressed in terms of the external potential. Within this formalism a simple proof is produced of the known theorem that the long-wavelength surface-plasmon frequency of such a system is independent of either the surface-electron density profile or the hydrodynamic dispersion effect. The theory is applied to the problem of interaction of a moving external point charge with a jellium metal surface. The surface-electron density profile is treated in one- and two-step models. Hydrodynamic dispersion effects as well as the effects of the surface diffuseness and of the finite electron velocity of the external charge on the dynamical image-charge interaction are discussed. The relevance of some of these theoretical results to certain experimental situations involving the interaction of a metal surface with electrodynamic probes is pointed out.

I. INTRODUCTION

Recently there has been a revival of interest in the hydrodynamic approach[1–8] to the problem of linear response in a bounded electron gas, in particular for jellium surfaces. This is partly because of the inherent mathematical and conceptual simplicity of the hydrodynamic model itself, but mostly due to the great difficulty associated with the application of conventional many-body theory[9–11] to finite systems. After the development of density-functional techniques[12–14] by Hohenberg, Kohn, and Sham (HKS), the static response of metallic surfaces has been fairly successfully treated by the HKS theory. But there has been no corresponding success in the problem of dynamic response of metal surfaces.

Most of the dynamic calculations can be divided into two categories—model calculations in which the surface-electron density contour or equivalently the surface potential is assumed to be of known, simple analytic form,[15] and formal calculations[16] of rather formidable mathematical complexity. In this work, we shall write surface response equations of rather general nature and then discuss their applications to some simple model systems.

Electrodynamic response of a bounded electron gas has important implications for the interaction of a simple metal surface with electromagnetic probes. Examples of experimental situations where electrodynamic response of metal surface plays a significant role are very many: Low-energy-electron diffraction (LEED), fast-electron energy-loss spectroscopy, photoelectron spectroscopy, positron scattering, photon-assisted tunneling, desorption, reflection-electron-energy-loss (REEL) spectroscopy, optical reflectivity, and ion scattering spectroscopy are some of these techniques. For many of these experimental situations, effect of retardation (keeping the velocity of light finite) is not important (optical reflection and transmission experiments being the glaring exceptions). In this paper we concentrate on the nonretarded limit of the electrodynamic response, leaving inclusion of retardation effects in specific experimental situations for future publications. In particular, we apply the general formalism for a specific calculation of dynamical image interaction energy near a metal surface. This problem is of particular relevance to experimental techniques such as core-level spectroscopy,[17] low-energy electron diffraction,[18] positron scattering[19] (and possible formation of positron bound state) and electron-energy-loss spectroscopy.[20] The static screening of a point charge embedded near a metal surface can be successfully treated[21] by the density-functional theory as pro-

pounded in the HKS formalism. Hydrodynamic theory is basically a *quasistatic* generalization[5] of the simplest density-functional formalism for the *static* response of an inhomogeneous electron gas. As such, it is expected that the hydrodynamic model will give a reasonable qualitative description of the dynamic interaction between a moving point charge and a bounded electron gas. In fact, indications of the usefulness of the hydrodynamic model in describing the dynamical response of a metal surface already exist in the form of the ability of this model in producing qualitatively correct dispersion relations for the surface plasmons[1,4] in simple metal surfaces and for the interface plasmons[8] in simple bimetallic interfaces.

One important feature of the hydrodynamic model makes it particularly attractive for the kind of qualitative description of the dynamical surface response we are seeking in this paper. This is its relative simplicity. It provides an insight into the physical behavior of the system that is sometimes absent in a more microscopic approach [such as detailed random-phase-approximation (RPA) calculations[10]], which must involve heavy numerical computations from the beginning. This relative simplicity and the physical approach of the hydrodynamic model also make it possible for one to apply the technique to metal surfaces described by electron density profiles, which are more realistic than the simple step-density approximation used extensively in the literature. In this paper we consider a surface-electron density profile (the so-called "two-step" model[3,8]), which is more realistic than the step-density approximation adopted in many papers[2,7] on surface dynamic response.

The general plan of the paper is the following: In Sec. II, we use a hydrodynamic model to derive the general equations governing the electromagnetic response of metal surfaces under the jellium background approximation. In Sec. III we take the nonretarded limit of the response equation and obtain the longitudinal response equations in its most general form. We give a simple analytic proof of the general theorem[22–24] that in the long-wavelength limit the regular surface plasma frequency is $\omega_p/\sqrt{2}$, independent of the surface-electron density profile, where ω_p is the bulk-plasma frequency. That the long-wavelength surface plasma frequency is independent of the surface-electron density profile was first shown[22] by Feibelman within a RPA model. Eguiluz, Ying, and Quinn proved[23] this theorem within a hydrodynamic model, employing a technique that is very different from what has been employed in this work. In Sec. IV we discuss a simple application of the formalism developed in Secs. II and III by calculating the dynamical interaction of a moving point charge with a metal surface. The surface-electron density profile is treated within two models: a sharp one-step model and a diffuse two-step model. We conclude in Sec. V by providing a summary and critique of our results.

II. ELECTROMAGNETIC RESPONSE OF METAL SURFACES

The constitutive relation connecting the induced particle current $\vec{J}$ in the system and the total local self-consistent electric field $\vec{E}$ can be written as

$$\vec{J}(\vec{k},\omega)=\int \frac{d^3k'}{(2\pi)^3}\overleftrightarrow{\sigma}(\vec{k},-\vec{k}';\omega)\vec{E}(\vec{k}',\omega)\ , \quad (1)$$

where $\overleftrightarrow{\sigma}$ is the conductivity tensor. For mathematical convenience, we shall be working in the $(\vec{k},\omega)$ space. Note that in writing Eq. (1) translational symmetry has not been assumed in any direction. The expression for $\overleftrightarrow{\sigma}$ in the simplest hydrodynamic model has been derived before[4,8]—the i-j component of $\overleftrightarrow{\sigma}$ is given by

$$\sigma_{ij}(\vec{k},-\vec{k}';\omega)=-\frac{i}{\omega}n_0(\vec{k}-\vec{k}')\delta_{ij} -\frac{i\beta^2}{\omega}n_0(\vec{k}-\vec{k}')\frac{k_ik_j}{\omega^2-\beta^2k^2}\ . \quad (2)$$

We take $\hbar=m=e=1$ throughout this paper. In Eq. (2), $n_0(\vec{k}-\vec{k}')$ is the Fourier transform of the static equilibrium electron-density profile $n_0(\vec{r})$ of the system, β^2 is the coefficient of the hydrodynamic pressure term in the Euler equation, and δ_{ij} is the Kronecker δ function. We assume $n_0(\vec{r})$ to be arbitrary except that it depends only on the z coordinate which is taken to be normal to the surface plane. Thus, translational invariance is broken only in one direction. This makes

$$n_0(\vec{k}-\vec{k}')=(2\pi)^2n_0(k_z-k_z')\delta(\vec{q}_{||}-\vec{q}_{||}')\ ,$$

where $\vec{q}_{||},\vec{q}_{||}'$ are two-dimensional wave vectors parallel to the plane of the interface. The δ function in $\vec{q}_{||}$ assures that it is a conserved quantity, and Eq. (2) can be rewritten as

$$\sigma_{ij}(k_z,k_z')=-\frac{i}{\omega}n_0(k_z-k_z')\delta_{ij}(2\pi)^2\delta(\vec{q}_{||}-\vec{q}_{||}')-\frac{i\beta^2}{\omega}n_0(k_z-k_z')(2\pi)^2\delta(\vec{q}_{||}-\vec{q}_{||}')\frac{k_ik_j}{\omega^2-\beta^2q_{||}^2-\beta^2k_z^2}\ . \tag{3}$$

We shall from now on suppress the explicit $(\vec{q}_{||},\omega)$ dependence in various functions for the sake of brevity.

Electromagnetic response equations are obtained by combining the constitutive relation [Eq. (1)] with the full set of Maxwell's equations. Eliminating the magnetic field from Maxwell's equations, one obtains

$$E_i(\vec{k},\omega)=\frac{4\pi i}{\omega(\omega^2-c^2k^2)}(\omega^2\delta_{ij}-c^2k_ik_j)J_j(\vec{k},\omega)\ . \tag{4}$$

We are using the convention that a sum is implied over repeated indices. Combining Eqs. (4) and (1) with Eq. (3), we get a set of one-dimensional integral equations describing the electromagnetic response in the system. We consider p polarization $\vec{E}\equiv(E_x,0,E_z)$ to be specific, and also choose our axes such that $\vec{q}_{||}\equiv(q,0)$, without any loss of generality. It is then straightforward to write down the general integral equations satisfied by the total local self-consistent field $\vec{E}(\vec{k})$:

$$E_x(k_z)=A_{11}(k_z)\int_{-\infty}^{+\infty}\frac{dk_z'}{2\pi}n_0(k_z-k_z')E_x(k_z')+A_{12}(k_z)\int_{-\infty}^{+\infty}\frac{dk_z'}{2\pi}n_0(k_z-k_z')E_z(k_z')\ , \tag{5}$$

$$E_z(k_z)=A_{22}(k_z)\int_{-\infty}^{+\infty}\frac{dk_z'}{2\pi}n_0(k_z-k_z')E_z(k_z')+A_{21}(k_z)\int_{-\infty}^{+\infty}\frac{dk_z'}{2\pi}n_0(k_z-k_z')E_x(k_z')\ , \tag{6}$$

where

$$A_{11}(k_z)=\frac{4\pi(\omega^2-c^2q^2-\beta^2k_z^2)}{(\omega^2-c^2q^2-c^2k_z^2)(\omega^2-\beta^2q^2-\beta^2k_z^2)}\ , \tag{7}$$

$$A_{22}(k_z)=\frac{4\pi(\omega^2-c^2k_z^2-\beta^2q^2)}{(\omega^2-c^2q^2-c^2k_z^2)(\omega^2-\beta^2q^2-\beta^2k_z^2)}\ , \tag{8}$$

$$A_{12}(k_z)=\frac{4\pi(\beta^2-c^2)qk_z}{(\omega^2-c^2q^2-c^2k_z^2)(\omega^2-\beta^2q^2-\beta^2k_z^2)}=A_{21}(k_z)\ . \tag{9}$$

Once a choice for $n_0(z)$ [which determines $n_0(k_z-k_z')$] is made, the pair of coupled singular integral equations (5) and (6) must be solved to obtain the self-consistent electric fields. One can decouple Eqs. (5) and (6) to obtain two singular integral equations for the individual electric field components.

The pair of equations (5) and (6) represent the most general form of electromagnetic response in translationally noninvariant systems that include the nonlocal effects associated with the hydrodynamic dispersion. Harris and Griffin[24] first wrote a pair of equations that are equivalent to (5) and (6) in the context of a high-frequency limit of the RPA. Since all nonlocal effects are lost in the high-frequency RPA expansion, our response equations are more general and reduce to the equation of Harris and Griffin if we set $\beta=0$ in Eqs. (5) and (6). These equations are generalizations of those written down in Ref. 4 in the context of surface collective oscillations.

To express Eqs. (5) and (6) as more standard response equations connecting induced current with the external field, we make the self-consistent field approximation

$$\vec{E}(k_z)=\vec{E}_{ex}(k_z)+\vec{E}_{in}(k_z)\ , \tag{10}$$

where $\vec{E}_{ex}(k_z)$ is the external perturbing field and $\vec{E}_{in}(k_z)$ is the screening field induced in the bounded electron gas.

The induced field $\vec{E}_{in}(k_z)$ is now expressed in terms of induced scalar $\phi_{in}(k_z)$ and vector $\vec{A}_{in}(k_z)$ potentials. The scalar and vector potentials, on the other hand, can be written in terms of the induced density fluctuation $n(k_z)$ and the induced current density $\vec{J}(k_z)$. Doing this we get the following equations for the components of the self-consistent field:

$$\vec{E}(k_z)=\vec{E}_{ex}(k_z)+\frac{4\pi i\omega}{\omega^2-c^2k^2}\vec{J}(k_z)-\frac{4\pi ic^2}{\omega^2-c^2k^2}\vec{q}n(k_z)\,, \tag{11}$$

where $k^2=k_z^2+q^2$. The electron density and current fluctuations are related by the equation of continuity, which reads $\vec{q}\cdot\vec{J}=\omega n$ in the $(\vec{k},\omega)$ space. Using Eqs. (10) and (11) in the response equations (5) and (6) and doing some rearrangement of terms, we get

$$\int_{-\infty}^{+\infty}dk_z'\,[K_{1x}(k_z,k_z')J_x(k_z')+K_{1z}(k_z,k_z')J_z(k_z')]=F_x^{ex}(k_z) \tag{12}$$

and

$$\int_{-\infty}^{+\infty}dk_z'\,[K_{2x}(k_z,k_z')J_x(k_z')+K_{2z}(k_z,k_z')J_z(k_z')]=F_z^{ex}(k_z)\,. \tag{13}$$

In obtaining Eqs. (9) and (10) we have used the equation of continuity to eliminate the induced density fluctuation $n(k_z)$. The kernels K_{1x}, K_{2x}, K_{1z}, and K_{2z} depend on the functions A_{11}, A_{22}, and A_{12} [defined in Eqs. (7)–(9)] and on $n_0(k_z-k_z')$. These kernels are shown in the Appendix. The source terms $F_{x,z}^{ex}(k_z)$ depend on the external electric field and are given by

$$F_x^{ex}(k_z)=-E_x^{ex}(k_z)+A_{11}(k_z)\int_{-\infty}^{+\infty}dk_z'\,n_0(k_z-k_z')E_x^{ex}(k_z')+A_{12}(k_z)\int_{-\infty}^{+\infty}dk_z'\,n_0(k_z-k_z')E_z^{ex}(k_z') \tag{14}$$

and

$$F_z^{ex}(k_z)=-E_z^{ex}(k_z)+A_{22}(k_z)\int_{-\infty}^{+\infty}dk_z'\,n_0(k_z-k_z')E_z^{ex}(k_z')+A_{12}(k_z)\int_{-\infty}^{+\infty}dk_z'\,n_0(k_z-k_z')E_x^{ex}(k_z')\,. \tag{15}$$

Note that Eqs. (12) and (13) are a pair of coupled integral equations that describe the true system response to the external field. A general solution to Eqs. (12) and (13) will give the induced current $\vec{J}\equiv(J_x,0,J_z)$ in terms of the external field $\vec{E}_{ex}\equiv(E_x^{ex},0,E_z^{ex})$. The general method to solve this kind of singular, integral equation is quite complex.[25] We will just state here that a *formal* solution to the coupled integral equations (12) and (13) can be obtained[26] by applying the hydrodynamic boundary condition that the current $\vec{J}(k_z)$ is analytic in the upper half of the complex k_z plane [which follows from the condition that $\vec{J}(z)=0$ for $z>0$ where $z=0$ is taken to be the surface plane]. Since the formal solution does not elucidate the physics of the surface electrodynamic response and is a purely mathematical result of limited physical applicability, we do not pursue this solution in any detail here. We are content with the statement[26] that within the hydrodynamic model, an exact, formal solution of the problem of surface electromagnetic response indeed exists *provided* the hydrodynamic boundary condition [i.e., $\vec{J}(z)=0$ for $z>0$] can be assumed.

In the next section we consider the nonretarded $(c\to\infty)$ limit of Eqs. (12) and (13) in detail and work out specific applications for model systems.

III. NONRETARDED $(c\to\infty)$ LIMIT OF HYDRODYNAMIC RESPONSE

In this section we take the nonretarded limit of the formalism developed in Sec. II, thus restricting ourselves to the longitudinal response only. One can do this by taking the $c\to\infty$ limit of the general response equations (12) and (13) and using equation of continuity. The longitudinal response of the bounded electron gas is completely specified in terms of a single equation connecting the induced linear electron density fluctuation, $n(k_z)$, and the external potential, ϕ_e, describing the external longitudinal electric field $\vec{E}(k_z)$. Thus we introduce the following relations and then take the $c\to\infty$ limit of Eqs. (12) and (13):

$$E_x^{ex}(k_z)=-iq\phi_e(k_z)\,, \tag{16}$$

$$E_z^{ex}(k_z)=-ik_z\phi_e(k_z)\,, \tag{17}$$

$$qJ_x+k_zJ_z=\omega n(k_z)\,. \tag{18}$$

The last equation is just the equation of continuity in the $(\vec{k},\omega)$ space. After some straightforward algebra both Eqs. (12) and (13) yield the same following relationship [in the $(c\to\infty)$ limit] between the induced density fluctuation and the external potential:

$$n(k_z)-\left[\frac{4\pi}{\omega^2-\beta^2q^2-\beta^2k_z^2}\right]\int\frac{dk_z'}{2\pi}\frac{q^2+k_zk_z'}{k_z'^2+q^2}n_0(k_z-k_z')n(k_z')$$
$$=\left[\frac{k_z^2+q^2}{4\pi}\right]\phi_e(k_z)-\frac{1}{\omega^2-\beta^2q^2-\beta^2k_z^2}\int\frac{dk_z'}{2\pi}(q^2+k_zk_z')n_0(k_z-k_z')\phi_e(k_z')\,. \quad (19)$$

Equation (19) is the fundamental longitudinal response equation of a metal surface within hydrodynamic approximation connecting the external scalar potential ϕ_e with the induced electron density fluctuation n. To solve the response equation [Eq. (19)] we need boundary conditions which are provided by choosing a model for the equilibrium surface electron density profile such that $n_0(z)=0$ for $z>0$. This ensures that the linear density fluctuation $n(z)$ also vanishes outside the metal surface [i.e., $n(z)=0$ for $z>0$ in this model]. To discuss solutions of Eq. (19) we make the following specific model for the equilibrium surface-electron density profile;

$$n_0(z)=\begin{cases}n_0(1-e^{az}) & \text{for } z<0\,,\\ 0 & \text{for } z>0\,.\end{cases} \quad (20)$$

Thus the electron density is restored to the bulk value deep inside the metal ($z\to-\infty$) in an exponential fashion. This is very similar to the self-consistent surface-electron density profiles of metals obtained by Lang and Kohn.[27] The Friedel oscillations are absent in this model. It is well known that such oscillations do not arise within a Thomas-Fermi model.

Taking the Fourier transform of Eq. (20) and setting it for $n_0(k_z-k_z')$ in Eq. (19), we get

$$n(k_z)+\frac{4\pi in_0}{\omega^2-\beta^2(q^2+k_z^2)}\int\frac{dk_z'}{2\pi}\frac{q^2+k_zk_z'}{q^2+k_z'^2}\left[\frac{1}{k_z'-k_z-i\delta}+\frac{1}{k_z'-k_z-ia}\right]_{\delta\to0+}n(k_z')=F(k_z)\,, \quad (21)$$

where

$$F(k_z)=\frac{k_z^2+q^2}{4\pi}\phi_e(k_z)+\frac{in_0}{\omega^2-\beta^2q^2-\beta^2k_z^2}\int\frac{dk_z'}{2\pi}(q^2+k_zk_z')\left[\frac{1}{k_z'-k_z-i\delta}+\frac{1}{k_z'-k_z-ia}\right]_{\delta\to0+}\phi_e(k_z')\,. \quad (22)$$

Once an external potential $\phi_e(z)$ has been specified, $F(k_z)$ is completely known.

The integral equation (21) for the induced electron-density fluctuation $n(k_z)$ can be solved in a manner analogous to that suggested in Sec. II using the analyticity of $n(k_z)$ in the upper half of the complex k_z plane. Rather than pursuing the formal solution for $n(k_z)$ within the hydrodynamic model, we demonstrate one particular feature of the response equation (21). We show explicitly that Eq. (21) implies a self-sustained oscillation (collective mode) for the system at a long-wavelength frequency of $\omega_p/\sqrt{2}$ where $\omega_p=(4\pi n_0)^{1/2}$ is the bulk plasma frequency. This long-wavelength limit of surface plasma frequency is independent of the diffuseness of the surface and depends only on the uniform bulk electron density of the system.[22–24]

For collective modes ϕ_e and hence $F(k_z)$ are identically zero. Using that and doing an integration in the upper half of the complex k_z' plane [remembering $n(k_z')$ is analytic in upper half of k_z' plane] we get from Eq. (21)

$$n(k_z)=\frac{\omega_p^2}{\omega^2-\beta^2(q^2+k_z^2)}\left[-\frac{n(iq)}{2}\left[\frac{k_z-iq}{k_z-iq+ia}+1\right]+n(k_z)+\frac{q^2+k_z(k_z+ia)}{q^2+(k_z+ia)^2}n(k_z+ia)\right]\,, \quad (23)$$

where $\omega_p^2=4\pi n_0$ has been used. Setting $k_z=iq$ in Eq. (23) we get after some rearrangement of terms,

$$n(iq)=\frac{\omega_p^2}{\omega^2}\left[\frac{n(iq)}{2}+\frac{q}{a+2q}n(iq+ia)\right]\,. \quad (24)$$

Taking $q\to0$ limit of Eq. (31) we get

$$\omega^2=\tfrac{1}{2}\omega_p^2\,. \quad (25)$$

Thus we have demonstrated that this formalism

indeed leads to the correct result[22–24] that the long-wavelength surface plasmon frequency is $\omega_p/\sqrt{2}$, independent of the electron density profile of the surface involved. We have also shown that this general result does not depend on the explicit application of hydrodynamic boundary conditions. This theorem follows only from charge conservation.[22–24] In addition to this general result, Eqs. (23) and (24) also imply that the dispersion corrections to the long-wavelength surface plasmon frequency at finite wave vector would depend on the electron-density profile of the surface.[4] Thus in an inhomogeneous Fermi system, the nonlocal effects due to spatial dispersion and inhomogeneity are coupled and they usually arise in the same order.[4,23,28]

Two other features of Eqs. (22)–(24) deserve comments. In general, Eq. (23) may have more than one solution implying there could be more than one localized collective mode in the system.[4,8,23] However for $a^{-1}=0$, i.e., for a sharp step-density surface profile, Eq. (23) can have just one solution at $\omega=\omega_p/\sqrt{2}$ in the $q\to 0$ limit. Thus a sharp surface has only one collective mode associated with it.[4,8,23] The other point is that Eqs. (23) and (24) by themselves are incapable of yielding information about the surface-plasmon dispersion relation. To obtain that, one must use the hydrodynamic boundary condition $J_z(z=0-)=0$.

IV. DYNAMICAL IMAGE CHARGE INTERACTION NEAR A METAL SURFACE

As an application of the formalism developed in the last section, we consider the problem of image interaction between a point charge and a metal surface. We assume the point charge to be moving with uniform velocity in a direction normal to the surface and neglect any recoil effects for simplicity. We also assume the point charge to be external to the metal for the sake of simplicity. However, the full dynamical effects of the interaction will be preserved in the calculation. The external charge density can be written as

$$\rho_{\rm ex}(\vec{r},t)=Q\delta(x)\delta(y)\delta(z-z_0+vt)\ . \tag{26}$$

The point charge is thus of strength Qe. It is assumed to be moving along the z axis with uniform velocity v, with z_0 giving its position at $t=0$. The metal is assumed to occupy the half space $z<0$. Since the charge is taken to be external to the metal, it is in the $z>0$ half space. One can of course consider the external charge crossing the metal surface within the same formalism. For $v>0$, Eq. (26) signifies a point charge moving toward the metal occupying the half space $z<0$ with the surface at $z=0$. We first consider the case of a sharp metal surface with a single-step electron-density profile $n_0(z)=n_0\Theta(-z)$. The corresponding potential in $(\vec{k},\omega)$ space $\phi_e(k_z)$ of Sec. III is easily obtained and found to be

$$\phi_e(k_z)=-\left.\frac{4\pi iQe^{i\omega z_0/v}}{v(k_z^2+q^2)(k_z+\omega/v-i\delta)}\right|_{\delta\to 0+}\ , \tag{27}$$

neglecting any retardation effect. The density fluctuation $n(k_z)$ induced by this external potential can be calculated using the method developed in Sec. III. It is found to be

$$n(k_z)=\frac{A\omega_p^2}{2\beta^2(k_z^2+\gamma^2)}+\frac{iQe^{i\alpha z_0}(\omega^2-\beta^2q^2-\beta^2k_z^2)}{v\beta^2(k_z^2+\gamma^2)(k_z+\alpha-i\delta)}-\frac{iQ\omega_p^2e^{i\alpha z_0}}{2v\beta^2(k_z^2+\gamma^2)(\alpha+iq)}\ , \tag{28}$$

where $\alpha=\omega/v$. In Eq. (28), $\omega_p^2=4\pi n_0$ is the bulk plasma frequency of the metal and γ^2 is given by

$$\beta^2\gamma^2=\omega_p^2-\omega^2+\beta^2q^2\ . \tag{29}$$

The unknown constant A in Eq. (28) is to be obtained by the application of hydrodynamic boundary condition that the normal component of current density must vanish at the metal surface. It is straightforward but tedious to apply this boundary condition. The result of the calculation gives the following for the induced density fluctuation:

$$n(z)=\frac{Q\omega_p^2(\gamma+q)e^{\gamma z+i\alpha z_0}}{v(q+i\alpha)(2\gamma^2\beta^2+2\gamma q\beta^2-\omega_p^2)} \quad \text{for } z<0 \tag{30}$$

$$=0 \quad \text{for } z>0\ . \tag{31}$$

One can now obtain the dynamical-image interaction energy by calculating the induced potential ϕ_i due to $n(z)$ at the instantaneous position $(\vec{r}_{||}=0,\ z=z_0-vt)$ of the external charge. The dynamical image interaction energy is given by

$$V_i=\tfrac{1}{2}Q\phi_i(\vec{r}_{||}=0,\ z=z_0-vt,\ t)\ . \tag{32}$$

The potential ϕ_i in real space is given by

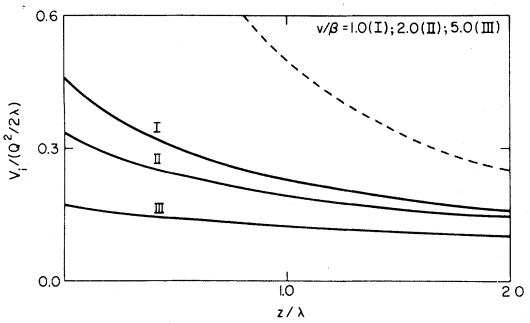

FIG. 1. Magnitude of dynamical image potential V_i as a function of distance z from a *one-step* surface for three different values of the velocity of the external point charge (with screening length λ kept constant). Also shown (dashed curve) is the classical result $V_i(z)=-Q^2/4z$ for the sake of comparison.

$$\phi_i(\vec{r}_{||},z,t)=\int \frac{d^2q}{(2\pi)^2}\int_{-\infty}^{+\infty}\frac{d\omega}{2\pi}e^{i\vec{q}\cdot\vec{r}_{||}-i\omega t}\phi_i(z)\ , \tag{33}$$

where $\phi_i(z)$ is given by

$$\phi_i(z)=-\frac{2\pi}{q}\int_{-\infty}^{0}dz'\,e^{-q|z-z'|}n(z')\ . \tag{34}$$

Using Eq. (30) in (34), one can get $\phi_i(z)$. Then from Eqs. (32) and (33) we finally obtain the following result for the dynamical image interaction energy:

$$V_i=-\frac{Q^2\omega_p^2}{4}\int_0^{\infty}dq\,e^{-2qz}F(q)\ . \tag{35}$$

The function $F(q)$ in Eq. (35) is given by

$$F(q)=[\tfrac{1}{2}\omega_p^2+\beta^2q^2+\beta q(\omega_p^2+\beta^2q^2+\beta^2v^2)^{1/2}+\beta^2v^2]^{-1}\ . \tag{36}$$

We summarize the salient features of V_i as follows.

(i) For $\beta=0$ and $v=0$, Eq. (35) gives the well-known electrostatic result

$$V_i=-\frac{Q^2}{4z}\ . \tag{37}$$

(ii) For small β and v one has the following asymptotic form for V_i:

$$V_i\approx-\frac{Q^2}{4z}\left[1-\frac{\lambda}{z}+\left[1-\frac{b^2}{\lambda^2}\right]\frac{\lambda^2}{z^2}+\cdots\right]\ , \tag{38}$$

where $\lambda=\beta/\omega_p$ is the screening length and $b=v/\omega_p$ is the natural length associated with the velocity of the external charge.

(iii) For $\beta=0$ and $z=0$ we get

$$V_i=-\frac{\pi Q^2}{4\sqrt{2}b}\ . \tag{39}$$

Thus the finite velocity makes the image potential nonsingular at the origin ($z=0$) even in the dispersionless limit ($\beta=0$).

Most of the above results for the image interaction for a single-step surface are known in the literature.[28,29] We have obtained the results here within a single, unified approach that treats both dynamics (finite v) and electron dispersion (finite β) on equal footing.

In Fig. 1 we show the magnitude of the image potential for a one-step electron density profile as a function of z/λ for three different values of the velocity v of the external charge. V_i has been plotted in units of $Q^2/2\lambda$. For the sake of comparison we have also shown the classical electrostatic result $-V_i=Q^2/4z$, which is divergent at $z=0$. Both hydrodynamic dispersion (by providing a length scale $\lambda=\beta/\omega_p$) and finite velocity v (by providing a length scale $b=v/\omega_p$) suppress the divergence of the classical result.

In a realistic system a third important length scale is provided by the diffuseness of the surface-electron density profile. In particular, the electron density $n_0(z)$ is expected[27] to drop from its bulk value n_0 to a value of zero over a finite distance a [see Eq. (20)]. This length a is typically of the order of the other two important lengths, λ and b, in the problem. We expect the diffuseness to have insignificant effect (and the single-step model to be reasonably good) only when $\lambda\gg a$. In order to study the quantitative effect of the surface diffuseness on the image potential we have employed the simplest model for the electron density profile that incorporates diffuseness. This is the two-step electron density profile that has been used[3,6,8,30] earlier in the literature. In this model the density profile for the bounded electron gas is taken to be

$$n_0(z)=n_1\Theta(-z-a)+n_2\Theta(-z)\Theta(z+a)\ . \tag{40}$$

Thus the bulk electron density has the uniform value n_1 whereas a small surface layer of thickness a has a density of n_2 ($<n_1$). The size a of the surface layer provides the diffuseness length scale and the electron density, instead of dropping to zero abruptly from the bulk value as in the single-

step model, goes to zero over a finite distance in two steps.

Application of the formalism developed in earlier sections to this model is straightforward, but quite tedious. Since the procedure is similar (but the details considerably more complicated) to that employed for the single-step density profile, we write only the final result for the dynamical image interaction energy V_i [Eq. (32)] between an externally moving point charge and the two-step surface (for $z \geq 0$):

$$V_i = -\frac{Q^2}{2}\int_0^\infty dq\, e^{-2q(z+a/2)}F_2(q) . \tag{41}$$

The function $F_2(q)$ for the two-step model is given by

$$F_2(q) = A\left[\frac{e^{-\gamma_2 a}}{q+\gamma_1}+\frac{e^{qa}}{q+\gamma_2}-\frac{e^{-\gamma_2 a}}{q+\gamma_2}\right] + B\left[\frac{e^{\gamma_2 a}}{q+\gamma_1}+\frac{e^{qa}}{q-\gamma_2}-\frac{e^{\gamma_2 a}}{q-\gamma_2}\right], \tag{42}$$

where

$$\gamma_1 = \left[\frac{1}{\lambda_1^2}+q^2\left[1+\frac{v^2}{\beta^2}\right]\right]^{1/2},$$
$$\gamma_2 = \left[\frac{1}{\lambda_2^2}+q^2\left[1+\frac{v^2}{\beta^2}\right]\right]^{1/2}. \tag{43}$$

The functions A and B in Eq. (49) are given by

$$A = \frac{f_+ e^{-qa}-g_+}{f_- g_+ - f_+ g_-} , \tag{44}$$

$$B = \frac{g_- - f_- e^{-qa}}{f_- g_+ - f_+ g_-} , \tag{45}$$

where

$$f_\pm = \frac{e^{(\pm\gamma_2-q)a}}{q+\gamma_1}+\frac{1-e^{(\pm\gamma_2-q)a}}{q\pm\gamma_2}\pm\frac{2\gamma_2\beta^2}{\omega_{p2}^2} , \tag{46}$$

$$g_\pm = \frac{e^{\pm\gamma_2 a}}{q+\gamma_1}+\frac{e^{-qa}-e^{\pm\gamma_2 a}}{q\pm\gamma_2} - \frac{2\beta^2}{\omega_{p1}^2-\omega_{p2}^2}(\pm\gamma_2+\gamma_1)e^{\pm\gamma_2 a} , \tag{47}$$

with

$$\omega_{p1,p2}^2 = 4\pi n_{1,2} . \tag{48}$$

In Eq. (43), the screening lengths $\lambda_{1,2}$ are defined as before by $\lambda_{1,2}=\beta^2/\omega_{p1,p2}^2$. We have used the same electronic compressibility β to describe both the bulk system and the surface layer. This is a nonessential approximation made mainly to keep the number of parameters at its minimum. We have verified that the introduction of different compressibilities for the bulk and the surface layer has insignificant quantitative effect on our results.

Before presenting our numerical results for the image energy V_i given by Eq. (41), we comment upon an important aspect of the calculation. Taking the $a \to 0$ limit of Eqs. (41)–(47), one recovers the result [Eqs. (35) and (36)] for the one-step model as one should since the two-step model reduces to the one-step model in the $a=0$ limit.

In Figs. 2–5 we show the functional dependence of the magnitude of the image potential V_i for the two-step model on various parameters (a, v, λ_2, and λ_1) of the theory by numerically evaluating the integral on the right-hand side of Eq. (41). In Fig. 2 we depict the variation of $-V_i/(Q^2/2\lambda_1)$ as a function of z/λ_1 for four different values of a with the other parameters kept constant. Results for $a=0$, λ_1, $2\lambda_1$, and $4\lambda_1$ are shown and $-V_i$ goes down in magnitude with the increase in the diffuseness of the surface profile. As expected, the result for the two-step model with $a=0$ is the same as the corresponding result for the one-step model. In Fig. 3 we have shown the variation of V_i with z for four different values of the velocity of the external point charge. The top curve (labeled I) is for $v=0$. In Fig. 4 we show the variation of V_i with z for two different values of λ_2 keeping λ_1, a, and v constant. It turns out that results for $\lambda_2 > 7.5\lambda_1$ are not much different from that shown in curve I in Fig. 3. Finally, in Fig. 5 we show the dependence of $V_i(z)$ on λ_1 itself by plotting $-V_i(z)$ against z for fixed a, λ_2, and v but

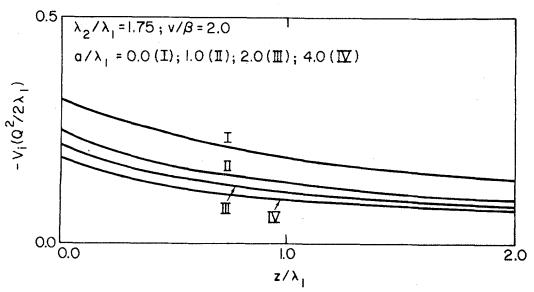

FIG. 2. Magnitude of dynamical image potential V_i as a function of distance z from a *two-step* surface for four different values of the surface diffuseness parameter a (with the other parameters λ_1, λ_2, v, and β being constant). Curve I (with $a=0$) is the same as the corresponding one-step model result (Fig. 1).

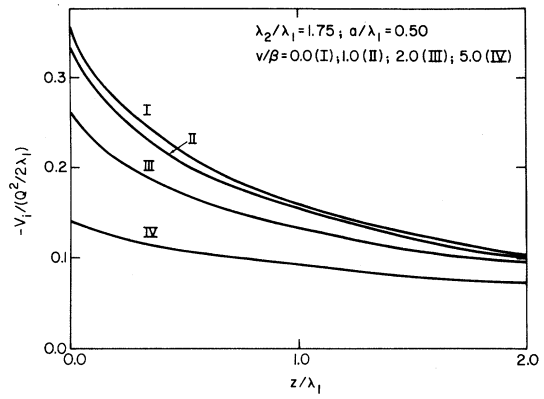

FIG. 3. Magnitude of dynamical image potential V_i as a function of distance z from a *two-step* surface for four different values of the velocity of the external charge including that for the pure static ($v=0$) case (curve *I*). All the other parameters (a, λ_1, λ_2, and β) have been kept constant.

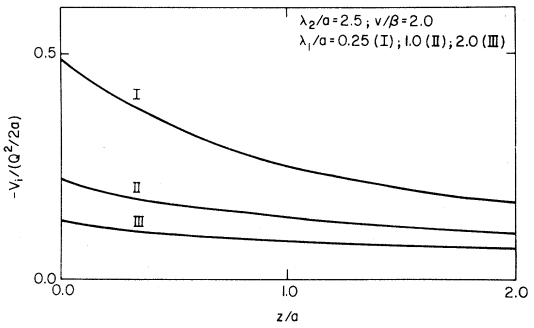

FIG. 5. Magnitude of dynamical image potential V_i as a function of distance z from a *two-step* surface for three different values of the screening length λ_1 of the bulk system. Other parameters (a, λ_2, v, and β) have been kept constant. The length and energy units for this figure are different from the other four figures as shown.

for three different values of λ_1. We point out that Fig. 5 has different length (measured in units of a) and energy (measured in units of $Q^2/2a$) scales compared with the other four figures.

These four figures (Figs. 2—5) clearly illustrate the functional dependence of $V_i(z)$ on the different length scales (λ_1, λ_2, a, and $b=v/\omega_p$) of the two-step model. As we would expect, $V_i(z)$ does not depend too sensitively on λ_2. However, its dependence on the other three lengths (λ_1, a, and b) is quite strong and any one of these three lengths by itself is sufficient to saturate $V_i(z=0)$ suppressing the divergence of the classical-image potential. In spite of its simplicity, one expects the qualitative features of the two-step model (as illustrated in Figs. 2—5) to remain valid in more realistic diffuse density profiles for metal surfaces. Thus we have demonstrated through two examples how the formalism can be applied to study interaction of external probes with metal surfaces.

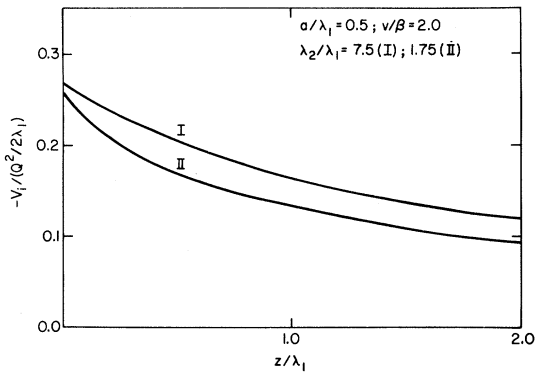

FIG. 4. Magnitude of dynamical image potential V_i as a function of distance z from a *two-step* surface for two different values of the screening length λ_2 of the surface layer. Other parameters (a, λ_1, v, and β) have been kept constant.

V. CONCLUSION

In this paper we have developed a formal hydrodynamical approach to the problem of dynamical response of bounded electron gas to external electromagnetic perturbation. The approach uses the simple and physically appealing hydrodynamical model to include nonlocal effects of spatial dispersion, as opposed to more complicated microscopic, many-body theories. It should be emphasized that the nonlocal effects associated with hydrodynamic dispersion are retained in the theory only by virtue of the compressibility β of the electron gas being finite. Nonlocal effects are eliminated on setting $\beta=0$. This can be easily seen from the earlier sections of the paper by noting that the two-dimensional wave number q always enters in the combination βq, and thus setting $\beta=0$ eliminates all nonlocality. The reverse, however, is not true. Thus one can consider the long-wavelength limit of the theory by taking the limit $q\to 0$ and still preserve effects of hydrodynamical dispersion through the normal z direction. One effect of such hydrodynamic dispersion is the recently discussed[1,4,8,23] higher multipole-collective modes associated with nonabrupt metal surfaces in which the surface-electron density profile goes to zero

smoothly over a distance, in contrast to the step-density model employed in many approximations. These modes have a well-defined long-wavelength limit,[4] but would disappear under the approximation $\beta=0$. These modes thus exist only by virtue of hydrodynamic dispersion of a bounded electron gas. It is only fair to point out that higher multipole plasmons have not yet been observed experimentally. However, very recent calculations predict[30] the existence of coupled higher-multipole–optical-phonon modes in degenerate, polar semiconductor surfaces. These coupled "multipolaritons" lie in the infrared and seem to be more amenable to experimental observation.

Retention of nonlocality is reasonably easy within the hydrodynamical model as has been demonstrated explicitly in this paper. On the other hand, microscopic theories like the RPA become quite complicated and numerically very involved if one tries to keep nonlocal effects in the final results. Doing high-frequency expansion in microscopic theories and keeping only the leading order term are relatively simple. This procedure, however, excludes nonlocal effects from the result. One drawback of the hydrodynamic model is that the compressibility β is not correctly known within the formalism. We have kept it as a given constant in this paper, without specifying its exact value. One can specify[31] $\beta^2=\frac{3}{5}v_F^2$, where v_F is the Fermi velocity in the *bulk* by demanding that the bulk plasmon dispersion relation obtained within the hydrodynamical model be the same as that in RPA. However, there is no guarantee that the RPA form for plasmon dispersion is the exact form (as a matter of fact, one expects corrections to the RPA result due to local field effects), and therefore it may be more meaningful to take β^2 as a parameter in the hydrodynamic model that should be adjusted by comparing with experiment.

A specific application of the general theory worked out in Sec. IV of this paper is the problem of interaction of a fast moving point charge with a simple metal surface. As we have emphasized in the Introduction, this dynamical image interaction energy is of relevance to a number of experimental situations of interest in surface science. In particular, three mechanisms that suppress the unphysical divergence at $z=0$ of the *classical* image energy, $V_i=-Q^2/4z$, are discussed in terms of the quantitative results obtained for the one-step and the two-step electron density models for the surface. These mechanisms are the screening by the inhomogeneous electron gas, the diffuseness of the metal surface, and the finite velocity of the external point charge. To our knowledge this is the first calculation of the interaction between a point external charge and a metal surface within the hydrodynamical model that includes effects of hydrodynamic dispersion (screening), surface diffuseness and the finite velocity of the external charge. We have demonstrated through Figs. 1–5 that any one of these three physical effects by itself is sufficient to saturate the image potential at $z=0$. Each process provides a characteristic length scale described by λ, a, and b which are defined in Sec. IV of the paper. Actually, for the two-step model there are two screening lengths, λ_1 and λ_2, corresponding to the bulk and the surface-electron densities, respectively. But the parameter λ_1 has much more quantitative effect than λ_2 for the ranges of parameter values we have investigated.

It turns out (as can be seen from Figs. 1–5) that for large values of z, the image potential approaches the classical formula. However, depending on the actual magnitudes of the three-length scales λ, a, and b, the regime of validity of the classical image formula is shifted toward larger and larger values of z. The relative magnitudes of λ $(=\beta/\omega_p)$, b $(=v/\omega_p)$, and a (diffuseness length of the surface profile) could be quite different depending on the system and the experimental situation involved. For example, in simple metals (without any adsorbate) λ and a are expected to be of the order of a few angstroms at most. The parameter b, on the other hand, depends on the velocity of the external charge and could vary from the order of tens of Å (or lower) in LEED experiments to many times larger values in fast electron-energy loss experiments. In the latter situation this length scale clearly describes the dominant effect in the physics of image interaction. On the other hand, in a purely static situation (chemisorption, for example), b is zero and inclusion of λ and a in the analysis is essential. Our results from Sec. IV show that for comparable magnitudes of the length scales λ, a, and b, they are equally important in controlling the magnitude of the image-interaction energy. However, a formula of the Gomer-Swanson type[32] where we write

$$V_i(z)=-Q^2/4(z+\lambda+b+a/2)=-Q^2/4z_{\text{eff}}$$

works only when z_{eff} is very large.

A direct comparison between the theoretical results of this paper and experiments is not possible for a variety of reasons. For one thing very few experiments provide a direct measure of the image-interaction energy. Recent LEED measurements[18] report observation of the saturation of the

image potential at Cu(001) surface. However, jellium is expected to be a rather poor approximation for copper. This inhibits a direct comparison between our calculations and these experimental measurements. The basic experimental finding that for decreasing distance between the probe electrons and the metal surface, the image potential is progressively weaker than the classical value is totally consistent with our theoretical results. Also the importance of dynamics (finite external electron velocity) in such image-potential saturation is clearly illustrated by this experiment.[18] Inclusion of dynamics in the image-potential interaction is one of the important ingredients of this paper.

Two other types of experiments are important in providing information about the dynamical image-charge interaction near a metal surface. These are core-level spectroscopy[17,33] and positron scattering[19] from metal surfaces. The screening energy or the "extra-atomic relaxation energy" in the core-level spectroscopy is nothing but the image interaction energy calculated in the last section. In the positron-scattering experiment the important question of whether an image-potential—induced surface-bound state exists for positrons near a particular metal surface or not depends in a rather delicate manner on the actual shape of the image potential. Such questions have so far been dealt[19] within models that neglect the dispersion of the metallic electrons and the finite velocity of the positrons. Our work in this paper indicates that there could be corrections to the positron binding energy arising from these effects. However, we do not attempt any detailed comparison between the simple theory developed in this paper and actual experimental results. The theory and the numerical results obtained in Sec. IV should be taken as establishing important qualitative trends in the electromagnetic response of metal surfaces and in pointing out the relative quantitative significance of different physical effects. The actual results themselves should not be taken too seriously in view of the large number of rather simplifying approximations involved in the calculation.

ACKNOWLEDGMENTS

The author thanks Victor Korenman for a critical reading of the manuscript. He is grateful to the University of Maryland Computer Center for providing the computer time needed for the work. The work is supported in part by Grant No. NSF-DMR 79008819.

APPENDIX

We write down the kernels K_{1x}, K_{1z}, K_{2x}, and K_{2z} of the integral equations (16) and (17) in this appendix:

$$K_{1x}(k_z,k_z')=\frac{4\pi i(\omega^2-c^2q^2)}{\omega(\omega^2-c^2k_z^2-c^2q^2)}\delta(k_z-k_z')-\frac{4\pi i(\omega^2-c^2q^2)}{\omega(\omega^2-c^2k_z'^2-c^2q^2)}A_{11}(k_z)n_0(k_z-k_z')$$
$$+\frac{4\pi ic^2qk_z'}{\omega(\omega^2-c^2k_z'^2-c^2q^2)}A_{12}(k_z)n_0(k_z-k_z')\ . \tag{A1}$$

$$K_{1z}(k_z,k_z')=-\frac{4\pi ic^2qk_z}{\omega(\omega^2-c^2k_z^2-c^2q^2)}\delta(k_z-k_z')+\frac{4\pi ic^2qk_z'}{\omega(\omega^2-c^2k_z'^2-c^2q^2)}A_{11}(k_z)n_0(k_z-k_z')$$
$$-\frac{4\pi i(\omega^2-c^2k_z'^2)}{\omega(\omega^2-c^2k_z'^2-c^2q^2)}A_{12}(k_z)n_0(k_z-k_z')\ . \tag{A2}$$

$$K_{2x}(k_z,k_z')=-\frac{4\pi ic^2qk_z}{\omega(\omega^2-c^2k_z^2-c^2q^2)}\delta(k_z-k_z')+\frac{4\pi ic^2qk_z'}{\omega(\omega^2-c^2k_z'^2-c^2q^2)}A_{22}(k_z)n_0(k_z-k_z')$$
$$-\frac{4\pi i(\omega^2-c^2q^2)}{\omega(\omega^2-c^2k_z'^2-c^2q^2)}A_{12}(k_z)n_0(k_z-k_z')\ . \tag{A3}$$

$$K_{2z}(k_z,k_z')=\frac{4\pi i(\omega^2-c^2k_z^2)}{\omega(\omega^2-c^2k_z^2-c^2q^2)}\delta(k_z-k_z')-\frac{4\pi i(\omega^2-c^2k_z'^2)}{\omega(\omega^2-c^2k_z'^2-c^2q^2)}A_{22}(k_z)n_0(k_z-k_z')$$
$$+\frac{4\pi ic^2qk_z'}{\omega(\omega^2-c^2k_z'^2-c^2q^2)}A_{12}(k_z)n_0(k_z-k_z')\ . \tag{A4}$$

[1]A. J. Bennett, Phys. Rev. B 1, 203 (1970).
[2]J. Heinrichs, Phys. Rev. B 7, 3487 (1973).
[3]A. D. Boardman, B. V. Paranjape, and R. Teshima, Surf. Sci. 49, 275 (1975).
[4]A. Eguiluz and J. J. Quinn, Phys. Rev. B 14, 1347 (1976).
[5]S. C. Ying, Nuovo Cimento B23, 270 (1974).
[6]F. Forstmann and H. Stenschke, Phys. Rev. Lett. 38, 1365 (1977).
[7]A. Eguiluz, Phys. Rev. B 23, 1542 (1981).
[8]S. Das Sarma and J. J. Quinn, Phys. Rev. B 20, 4881 (1979).
[9]A. Bagchi, Phys. Rev. B 15, 3060 (1977).
[10]P. J. Feibelman, Phys. Rev. B 9, 5077 (1974), and references therein.
[11]P. J. Feibelman, C. B. Duke, and A. Bagchi, Phys. Rev. B 5, 2436 (1972).
[12]P. Hohenberg and W. Kohn, Phys. Rev. 136, 864 (1964).
[13]W. Kohn and L. J. Sham, Phys. Rev. 140, 1133 (1965).
[14]L. J. Sham and W. Kohn, Phys. Rev. 145, 561 (1966).
[15]Most of Refs. 1—10 fall in this category.
[16]S. Chakravarty, M. B. Fogel, and W. Kohn, Phys. Rev. Lett. 43, 775 (1979).
[17]J. W. Gadzuk, Surf. Sci. 67, 77 (1977).
[18]R. E. Dietz, E. G. McRae, and R. L. Campbell, Phys. Rev. Lett. 45, 1280 (1980).
[19]R. M. Nieminen and C. H. Hodges, Phys. Rev. B 18, 2568 (1978).
[20]H. Raether, in *Springer Tracts in Modern Physics,* edited by G. Höhler (Springer, Berlin, 1965), Vol. 38, p. 84, and references therein.
[21]S. C. Ying, J. R. Smith, and W. Kohn, J. Vac. Sci. Technol. 9, 575 (1971).
[22]P. J. Feibelman, Phys. Rev. B 3, 220 (1971).
[23]A. Eguiluz, S. C. Ying, and J. J. Quinn, Phys. Rev. B 11, 2118 (1975).
[24]J. Harris and A. Griffin, Phys. Rev. B 3, 749 (1971).
[25]N. I. Muskhelishvili, *Singular Integral Equations* (Noordhoff, Gronigen, Holland, 1953).
[26]S. Das Sarma (unpublished).
[27]N. D. Lang and W. Kohn, Phys. Rev. B 1, 4555 (1970).
[28]G. Barton, Rep. Prog. Phys. 42, 936 (1979).
[29]D. M. Newns, J. Chem. Phys. 50, 4572 (1969); R. Ray and G. D. Mahan, Phys. Lett. 41A, 301 (1972); J. Heinrichs, Phys. Rev. B 8, 1346 (1973).
[30]S. Das Sarma, J. J. Quinn, and A. Eguiluz, Solid State Commun. 38, 253 (1981).
[31]R. H. Ritchie, Prog. Theor. Phys. 29, 607 (1963).
[32]R. Gomer and L. W. Swanson, J. Chem. Phys. 38, 1613 (1963).
[33]A. M. Bradshaw, W. Domcke, and L. S. Cederbaum, Phys. Rev. B 16, 1480 (1977).